Chapter 9
Oregon Shelf Hypoxia Modeling

Andrey O. Koch, Yvette H. Spitz and Harold P. Batchelder

Abstract Bottom hypoxia on the shelf in the Northeast Pacific is caused by different processes than coastal hypoxia related to riverine inputs. Hypoxia off the coast of Oregon is a naturally occurring process as opposed to the anthropogenically forced hypoxia found in many coastal environments (e.g., Gulf of Mexico shelf, Chesapeake Bay). Off Oregon, bottom hypoxia occurs in summers that have large upwelling-driven near-bottom transport of high nitrate, low dissolved oxygen (DO) waters onto the shelf. The combination of low DO and high nitrate provides initially low (but not hypoxic) DO conditions near the bottom, and nitrate fertilization of shelf surface waters, leading to substantial phytoplankton production. Some production is grazed, and some of it sinks to the bottom where it decomposes consuming oxygen, creating bottom hypoxia in some years. Terrestrial runoff of nutrients into the system is small and not responsible for the development of bottom hypoxia. Similar processes contribute to natural hypoxia in other eastern boundary current upwelling regions, such as the Humboldt Current off Peru and the Benguela Current off Namibia and South Africa. We summarize the observational data on DO and illustrate the coupled bio-physical modeling of hypoxia that has been done on the Oregon shelf. We compare hypoxia development in summer of 2002 and 2006, which differed in timing, spatial extent and intensity of hypoxia. Sensitivity analysis using various initial and boundary conditions for nitrate and dissolved oxygen reveals some of the essential conditions responsible for hypoxia development on the Oregon shelf.

A.O. Koch (✉)
Department of Marine Science, University of Southern Mississippi, Hattiesburg, USA
e-mail: andreyokoch@gmail.com

Y.H. Spitz · H.P. Batchelder
College of Earth, Ocean, and Atmospheric Sciences, Oregon State University, Corvallis, USA
e-mail: yspitz@coas.oregonstate.edu

H.P. Batchelder
North Pacific Marine Science Organization, Sidney, BC, Canada
e-mail: hbatch@pices.int

D. Justic et al. (eds.), *Modeling Coastal Hypoxia*,
DOI 10.1007/978-3-319-54571-4_9

Keywords Oregon shelf · Natural hypoxia · Biophysical model of hypoxia · Observation-model comparisons · Interannual/seasonal variability

9.1 Introduction

Hypoxic regions in the world's oceans are becoming more numerous, lower in oxygen content, and expanding in area, volume and duration (Diaz and Rosenberg 2008). The concentration of dissolved oxygen (hereafter, DO) in coastal ocean regions is determined by air-sea exchange, ocean circulation, biological processes and anthropogenic activities. Hypoxia, defined by DO concentrations less than 1.43 ml L^{-1} (Grantham et al. 2004) and, in some cases, anoxia (DO < 0.5 ml L^{-1}; Chan et al. 2008) are known to occur in coastal regions, typically due to excessive nutrient input derived from agricultural runoff, or from waste management facilities incapable of handling the loads in regions of high human population density. The Louisiana–Texas shelf of the Gulf of Mexico (Chaps. 1, 3, 7, 8, 10, 13 and 14), the Chesapeake Bay (Chaps. 5, 6, 11 and 12), Narragansett Bay, RI (Chap. 4) and Green Bay, Lake Michigan (Chap. 2) are all regions that have experienced substantial anthropogenic nutrient enrichment and eutrophication as a primary contributing cause of hypoxia. Changes in DO include reductions in concentration, particularly near the bottom, seasonal extension of the duration or presence of hypoxia, and altered spatial patterns of hypoxia. Seasonal hypoxia is relatively common in semi-enclosed bays and estuaries where bottom waters have longer residence times due to reduced exchanges with more open regions. Summer is especially vulnerable to hypoxia development because stronger density stratification inhibits vertical exchange of surface and bottom waters, and high surface primary production creates organic detritus that sinks to bottom waters and remineralizes, consuming DO.

The open continental shelves of Oregon and Washington along the Pacific Northwest Coast have experienced a long-term (50 year) decline in late-summer DO (Chan et al. 2008), but without evidence of anthropogenic nutrient inputs and eutrophication. Instead, these shelves, and shelves more generally along eastern boundary currents, develop near-bottom hypoxia caused by natural oceanographic processes (Chan et al. 2008; Escribano and Schneider 2007).

The Pacific Northwest Coast experiences strong seasonally reversing winds. Winds during winter (October–April) are strongly from the SW, which causes onshore surface Ekman transport and downwelling of well-oxygenated surface waters on the inner to middle shelf. During this time, waters near the bottom on the central Oregon shelf are well oxygenated (ca. 4–7 ml L^{-1}). During spring winds change from predominantly northward to southward (spring transition). The timing of the spring transition and the duration of the summer upwelling season varies greatly from year to year, as illustrated by the along-shore wind data for the three years (2002, 2006 and 2008) considered in this study (Fig. 9.1 and Table 9.1). Strong, persistent southward winds in the summer lead to offshore Ekman transport of coastal surface waters. Coastal water is replaced by cold, upwelled, nutrient rich,

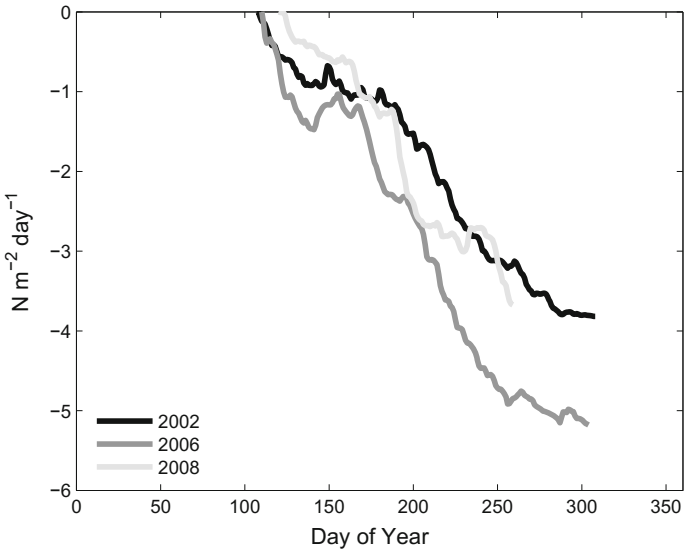

Fig. 9.1 Cumulative wind forcing (Nm^{-2} d^{-1}) for the upwelling season of 2002, 2006 and 2008. Note the later start and earlier end of upwelling in 2008, and the similar durations of upwelling in 2002 and 2006, but the 34% greater net upwelling during 2006. (Data retrieved from http://damp.coas.oregonstate.edu/windstress/index.html). April 1 is day of year 91; May 1 is day of year 121. November 1 is day of year 305

Table 9.1 Details of wind forcing for 2002, 2006 and 2008 from the National Data Buoy Center station 46050 located 20 nautical miles west of Newport, OR (station has a bottom depth of 137 m). See http://damp.coas.oregonstate.edu/windstress/index.html for summary of data

Year	2002	2006	2008
Year-day of spring transition	107	110	120
Number of upwelling days	144	143	104
Number of downwelling days	58	46	36
Length of upwelling season (days)	202	189	140
Sum of downwelling stress (N m^{-2} d^{-1})	1.03	1.13	0.72
Sum of upwelling stress (N m^{-2} d^{-1})	−4.84	−6.22	−4.38
Sum of stresses (N m^{-2} d^{-1})	−3.81	−5.09	−3.66
Proportion of days that were downwelling	0.29	0.24	0.26
Percent reduction in upwelling stress due to downwelling during upwelling period	0.21	0.18	0.16

but relatively oxygen poor water (Bakun 1990). Peterson et al. (2013) show that the source of upwelling water is from depths of 100–170 m off the shelf, where the DO is 1.5–3 ml L^{-1} (e.g., not hypoxic) in most years. The intermediate and deep water of the eastern North Pacific has been isolated from the atmosphere for ca. seven years due to global ocean circulation and has experienced substantial DO loss due

to remineralization of sinking organic matter (Ueno and Yasuda 2003). The DO of the source waters may vary interannually by up to 1.0 ml L^{-1} (Grantham et al. 2004; Peterson et al. 2013).

The shelf waters in years with lower DO in offshore source waters are poised to go hypoxic earlier during the summer, reach lower minimum DO levels and possibly have more spatially extensive hypoxic regions. Years of sustained summer upwelling, such as occurred in 2002 and 2006, elevate nutrients in the inner-shelf, fueling productivity and reducing near-bottom oxygen levels due to remineralization of sinking particulate organic carbon (Grantham et al. 2004; Wheeler et al. 2003; Fig. 9.2). Thus, the development of near-bottom hypoxia on the Oregon shelf may have several contributing factors: initially low dissolved oxygen in the upwelling source waters; higher nutrient concentrations that upwell into the euphotic zone stimulate higher phytoplankton productivity; and greater sinking and remineralization of in situ produced organic matter near the bottom (Wheeler et al. 2003).

9.2 Hypoxia Variability on the Oregon Shelf

Hypoxia development on the Oregon shelf is seasonal and linked with upwelling-favorable winds. Anthropogenic eutrophication is not a significant contributor to the development of near-bottom hypoxia on the shelf of Oregon (and Washington and Southern British Columbia) in the Pacific Northwest (Chan et al. 2008; Crawford and Pena 2013). Upwelling-favorable winds may occur at any time of the year, but winds are persistently upwelling favorable during the spring and summer. Near-bottom hypoxia intensifies with duration of upwelling following the spring transition (Huyer et al. 1979) and often peaks in intensity and spatial extent on the Oregon shelf during late summer (August–September). Cumulative upwelling-favorable wind stress varies significantly interannually (Fig. 9.1). Although later retrospective studies have revealed periods of bottom hypoxia on the Oregon shelf several decades ago, the extent and ecological impacts of bottom hypoxia were not fully appreciated until the summer of 2002, when video surveys from remote operated vehicles showed dead and dying fish and invertebrates on the central Oregon shelf (Grantham et al. 2004). Prior to 2002, few hydrographic surveys included measurements of dissolved oxygen, as low oxygen was not considered a common occurrence in Oregon shelf waters.

Cross-shelf sampling of the Newport Hydrographic Line (44.65° N) during August–September of 1998–2009 showed 6 years (2000, 02, 05, 06, 07, 09) with extensive cross-shelf bottom hypoxia (Fig. 9.2). A few years (1998, 99, 2001, 03 and 08) showed little to no bottom hypoxia. What is responsible for these differences? To address this, we first examine the physical conditions leading to the 2002, 2006 and 2008 patterns of hypoxia. We then describe the results of coupled biophysical models that simulated the ecosystem and oxygen conditions on the Oregon shelf during the 2002 and 2006 upwelling period.

Spring–summer upwelling in 2002 was fairly persistent, but not exceptionally strong, whereas 2002 was remarkable in having exceptionally low oxygen

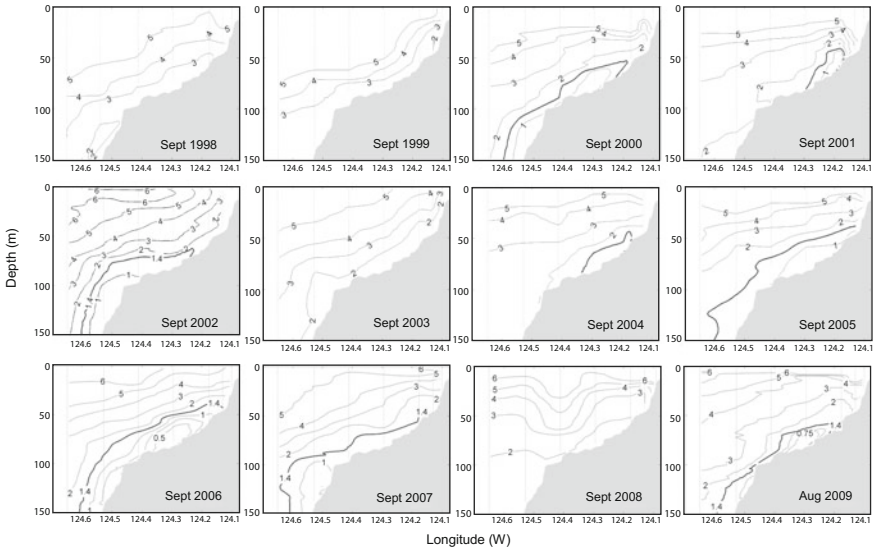

Fig. 9.2 Dissolved oxygen concentrations on the Newport Hydrographic transect in September (1998–2008) and August 2009 (lacking September data for 2009). Oxygen is contoured at 1 ml L^{-1} intervals for values of 1.0 or greater, and at 0.25 ml L^{-1} intervals where DO is less than 1 ml L^{-1}. An additional contour (*thick black line*) is shown at the hypoxic level of 1.4 ml L^{-1}. Figure provided courtesy of Bill Peterson (NWFSC, NOAA)

concentration and high nitrate concentrations in the water that upwelled from off the shelf (Fig. 9.3). In fact, the cumulative upwelling in 2002 was quite similar to 2008 (Fig. 9.1), a year in which bottom hypoxia was not prevalent. Oxygen concentrations shown by Grantham et al. (2004; their Fig. 4c) in July 2002 at 100–170 m at the shelf break off Newport, Oregon is very low, and far lower than the previously reported 95% confidence level from a decade of observations in the 1960s. Oceanic (offshore) regions of the Northeast Pacific have broad oxygen minimum zones (OMZ) at mid-depths. In 2002, the upwelled waters had very low DO (even below the hypoxic threshold in July), especially when compared to 2008 that was another "hypoxic" (though not strong) year (Fig. 9.2). The prevalence of hypoxic bottom conditions in 2002 was not recognized until the end of the summer, and there were few surveys during summer that included DO sampling in near-bottom water (Grantham et al. 2004).

During upwelling, high nutrient (especially nitrate), low oxygen waters upwell from depths of 100–200 m offshore (actual depth may vary interannually and seasonally; Peterson et al. 2013). The injection of nutrients into the photic zone enables high phytoplankton production on the shelf. In 2002, the higher nutrient concentrations resulted in shelf chlorophyll concentrations that were twice the levels of the preceding years 1998–2001 (Wheeler et al. 2003). Some of this phytoplankton production sinks as flocculates or fecal pellets to mid- and bottom waters on the shelf where it is remineralized, reducing near-bottom DO

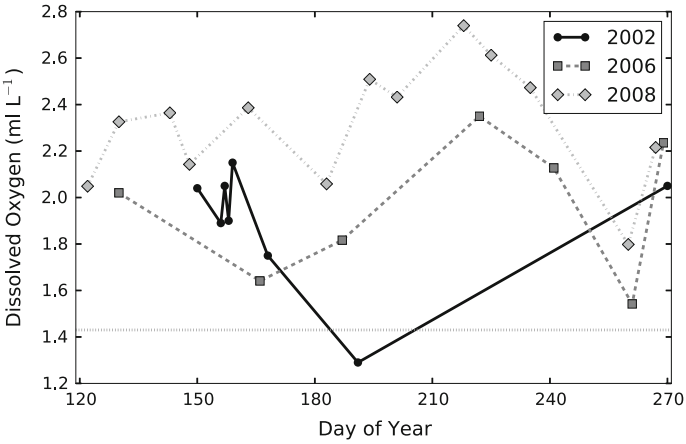

Fig. 9.3 Dissolved oxygen (DO) concentrations (ml L^{-1}) of the source water during the upwelling period (May–September) for 2002, 2006 and 2008. Source water DO concentrations were measured at the 26.44 sigma-t level at a station 25 miles off the coast of Newport Oregon (NH-25) as reported by Peterson et al. (2013). 2008 was a year of relatively little hypoxia on the Oregon shelf; 2002 and 2006 were years of widespread low DO on the shelf. (Data compiled by Jay Peterson, Oregon State University, from data collected by multiple sampling programs.)

concentrations even further from their initially low values. Gradually, the DO may be reduced below the hypoxia threshold.

Bottom DO is also strongly influenced by the local residence time of water (e.g., the near-bottom flow velocities and retention times), which may be controlled by bottom bathymetry (Castelao and Barth 2005). Wider continental shelves, complex bathymetries (bank complexes) and reduced wind stress (or intermittency of upwelling) lead to longer retention times, allowing greater localized consumption of DO (Barth et al. 2005; Hickey and Banas 2003). The region of most intense hypoxia in 2002 was associated with Heceta Bank, a wide region of the shelf, which has both sluggish flows and recirculation, and thus longer local retention times (Grantham et al. 2004; Barth et al. 2005).

The next few sections describe a physical–biological model applied to the Oregon shelf to understand the roles of physical and biological processes in modulating the development and extent of hypoxia. We focus on the summers of two hypoxic years, 2002 and 2006 that contrast in the severity and duration of their hypoxia.

9.3 Model of Oregon Shelf Hypoxia

We develop a coupled biological–physical model for the coastal ocean off Oregon (Fig. 9.4). We coupled a 3-km horizontal resolution Regional Ocean Modeling System (ROMS v3.0) physical model (Shchepetkin and McWilliams 2003, 2005) with a 5-component NAPZD (nitrate, ammonium, phytoplankton, zooplankton,

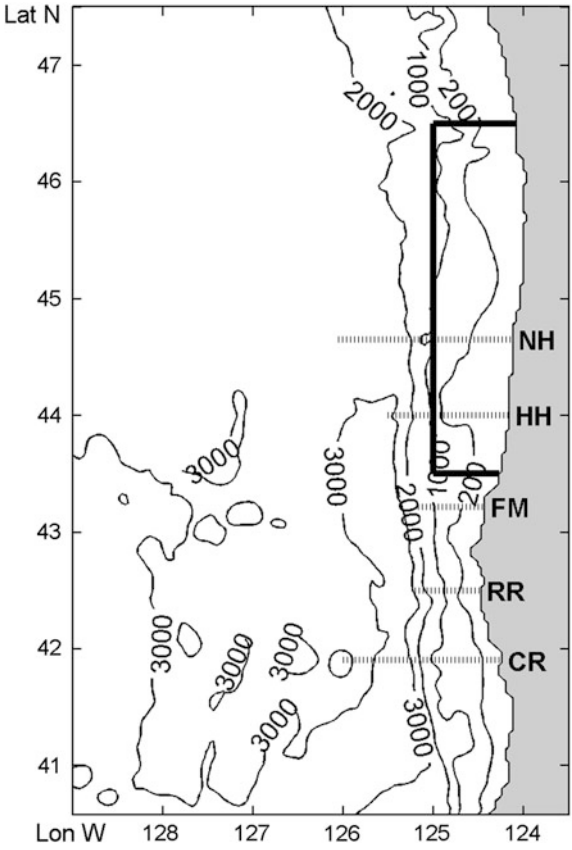

Fig. 9.4 Study location. The full region shown corresponds to the domain of the ROMS-CTZ Pacific Ocean model off Northern California (Southern end) to Northern Oregon (Northern end). The shelf region delimited by the *bold lines* (43.5–46.5° N) is the region analyzed in detail for bottom hypoxia. GLOBEC-LTOP observation locations on Crescent City (CR), Rogue River (RR), Five Miles (FM), Heceta Head (HH) and Newport Hydrographic (NH) transects are shown by *lighter dotted lines*. Bathymetry is shown by *thin numbered* (m) *lines*. The 200-m contour identifies the offshore edge of the shelf

detritus) ecosystem model (based on Spitz et al. 2005). The ROMS Coastal Transition Zone (ROMS-CTZ) computational domain spans 129–124° W meridionally and 40.5–47.5° N zonally and is identical to that used in Koch et al. (2010). Following their study, we simulate the period from April through August, which includes the transition in spring from northward winds to southward upwelling-favorable winds and summer upwelling circulation.

We add dissolved oxygen (DO) to the Spitz et al. (2005) NAPZD model to create a 6-component NAPZDO model (Fig. 9.5). DO is treated as a passive tracer with biologically mediated inputs (photosynthesis) and losses (zooplankton respiration, detritus remineralization and oxidation of ammonium), and an additional source (sink) term through air-sea exchange; the equations governing DO dynamics are shown in Appendix A. The computation of air-sea DO flux uses DO saturation concentration after Garcia and Gordon (1992) and gas transfer coefficient after Keeling et al. (1998). We do not explicitly simulate sediment-based DO consumption. Instead, we consider that settling particulate matter is retained within the bottom-most cell in the model and consumed there. We generate solutions for spring–summer of 2002 and 2006 that had extensive and severe hypoxia on the

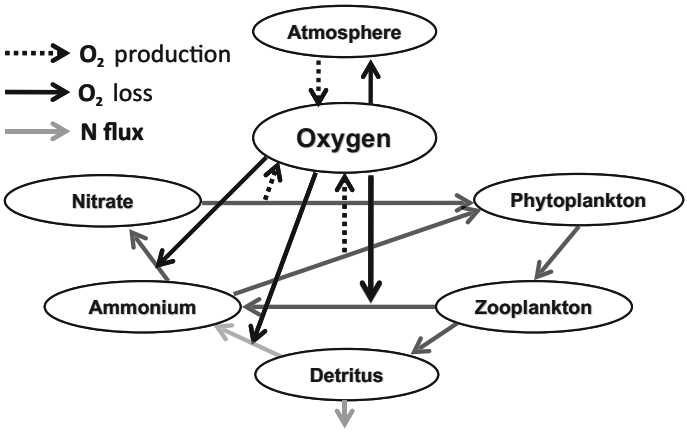

Fig. 9.5 Simple schematic of the ecological and dissolved oxygen model used for the Oregon shelf model. Model is modified from the ecosystem model of Spitz et al. (2005) to include dissolved oxygen processes as a passive tracer, with atmosphere exchange, biologically mediated inputs (*dotted black arrows*) and losses (*solid black arrows*). Nitrogen fluxes are shown with *solid gray arrows*

central Oregon shelf for most of the summer. The oxygen instantaneous values were saved twice-daily (every 12 h) for every grid cell.

9.3.1 Atmospheric Forcing, Initial and Open Boundary Physical Conditions

The coupled model simulations for 2002 are forced by 9-km horizontal resolution daily averaged COAMPS (The Coupled Ocean/Atmosphere Mesoscale Prediction System; Hodur 1997) winds and monthly averaged NCEP/NCAR (National Center for Environmental Prediction/National Center for Atmospheric Research; Kalnay et al. 1996) fields for heat-flux computation (shortwave solar radiation, air temperature, air pressure, relative humidity, precipitation) with 2.5° horizontal resolution. The simulations for 2006 were forced using 9-km atmospheric fields from the North American Mesoscale (NAM) model.

Initial conditions and open boundary conditions for velocities, temperature, salinity and sea surface height (SSH) were provided by a larger-scale NCOM-CCS (Navy Coastal Ocean Model for California Current System) model with 9-km horizontal resolution and 40 vertical levels: 20 sigma-levels (in upper 150 m) and 20 z-levels with constant depths (Shulman et al. 2004). Open boundary fields were provided daily. To suppress undesired effects of open boundary conditions as a result of merging larger-scale 9-km horizontal resolution NCOM fields with smaller-scale 3-km ROMS-CTZ fields we implemented a “sponge” layer that provided enhanced diffusivity and dissipation in the 100-km region adjacent to the

open boundaries. Our analysis of biological and DO fields was restricted to the subdomain from 43.5–46.5° N that excludes the sponge layer. The ROMS-CTZ domain along with the analysis subdomain is shown in Fig. 9.4.

9.3.2 Initial and Open Boundary Ecosystem Conditions

Providing the initial and boundary conditions for model runs requires knowledge of conditions in the real ocean, which is usually collected by multiple investigators. In our case, we relied extensively on field sampling conducted during the Global Ocean Ecosystems Dynamics (GLOBEC) Northeast Pacific regional program that sampled the Oregon shelf physics and ecosystem from 1997–2004 (especially the Long-Term Observation Program; hereafter LTOP), and subsequent sampling of the mid-to-late 2000s by individual investigators.

Open boundary conditions for nitrate, ammonia, phytoplankton, zooplankton and detritus are provided by the NCOM-CCS biological solutions for April–August of 2006 and 2008. NCOM simulations for 2002 did not include an ecosystem model, so for 2002 simulations using ROMS-CTZ we use biological boundary conditions from the NCOM-CCS simulation from 2008; wind forcing in 2008 was similar to wind forcing in 2002 (Fig. 9.1). NCOM's ecosystem includes two phytoplankton types (diatoms and nanoflagellates) and two zooplankton types (microzooplankton and mesozooplankton), with most of the biomass in the diatom and mesozooplankton types. Since our model had only a single phytoplankton and single zooplankton type, we used the sum of the multiple phytoplankton and zooplankton from NCOM-CCS for boundary conditions of ROMS-CTZ.

The initial nitrate conditions for the NCOM-CCS ecosystem model are based on Levitus World Ocean climatology (Levitus 1982). During the several decades long spin-up of NCOM-CCS, the nitrate fields showed significant drift and by the 2000s both the nitrate concentration and depth of the nitrocline had become biased (I. Shulman, personal communication). We eliminated the nitrate bias by adjusting the nitrate fields from NCOM using empirical linear regression between NCOM-CCS and GLOBEC-LTOP (Strub et al. 2002; Wetz et al. 2004) nitrate values taken at the same locations of the space–time domain for eight depth layers (0–50, 50–100, 100–150, 150–250, 250–350, 350–500, 500–700, 700 m-bottom). The bias correction was done separately for NCOM-CCS data from 2006 and 2008. GLOBEC-LTOP data on NO_3 and DO were collected at standard depths spanning from surface to 1000 m depth (or bottom, if shallower) along traditional Oregon observation lines: Crescent River (CR), Rogue River (RR), Five Miles (FM), Heceta Head (HH) and Newport Hydrographic (NH, Fig. 9.4) extending from the inner-shelf offshore to 126° W. Since the NCOM model did not include DO dynamics, we use a NO_3: DO linear regression to estimate the DO field from NO_3 for both boundary and initial conditions. The NO_3: DO linear relationship was more robust than other relations between DO and density, temperature or salinity. The linear regression ratio (slope −0.16, intercept 7.23) was derived using all

GLOBEC-LTOP NO_3 and DO observations from March–April of 1997–2004. The GLOBEC-LTOP observational program ended in 2004, but we assumed that the NO_3: DO relation derived from 1997–2004 applied also to 2006.

It is critical (as shown later by "Sensitivity analysis") that the simulation begin with realistic DO and NO_3 concentrations in order to accurately reproduce the shelf ecosystem dynamics, including hypoxia. This is why we took great care to provide accurate initial (i.e., early spring) spatially explicit NO_3 and DO fields. Initial DO and NO_3 for 2002 came from 2002 in situ LTOP data. For 2006, NO_3 came from the LTOP multi-year climatology. Initial spring 2006 DO came from a shelf-wide survey (J. Peterson, Oregon State University, unpublished data). Initial conditions for phytoplankton, zooplankton and detritus were provided from NCOM-2006 fields (for 2006) or NCOM-2008 (for 2002). Figure 9.6 summarizes the vertical

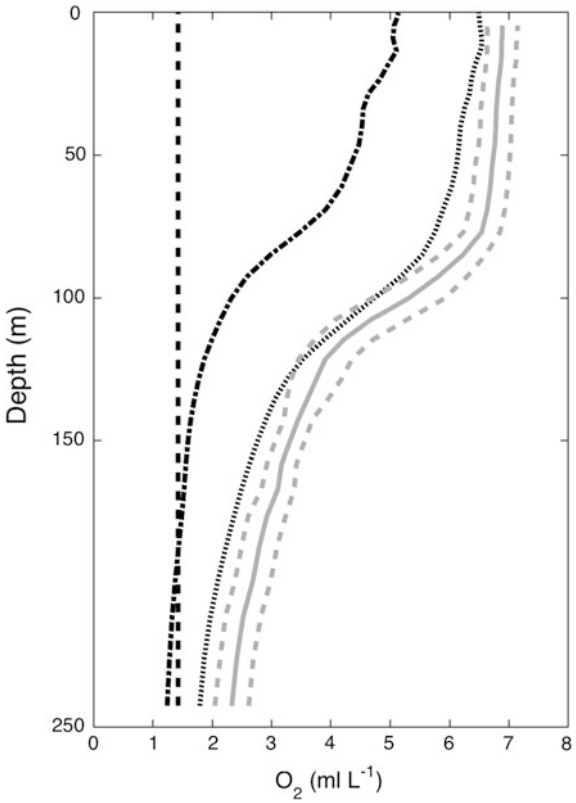

Fig. 9.6 Spring (March–April) dissolved oxygen concentration profiles at a location above the slope (25 nautical miles off the coast) along the Newport Hydrographic transect (see Fig. 9.1). The *dot-dashed black line* (LTOP2002) is the observed DO profile from the GLOBEC-LTOP cruise in 2002. The *dotted black line* (J.P. 2006) is the DO profile from the same location in 2006 (data provided by Jay Peterson, Oregon State University). The *solid gray line* is the mean climatological value from spring sampling at that station during 1998–2004 (including 2002), which is referred to as LTOP-clim in Table 9.2 and elsewhere in this chapter. The *dashed gray lines* about the climatological profile are 1 standard deviation above and below the mean. The hypoxia threshold of 1.43 ml L^{-1} is shown as the *black dashed vertical line*

profiles of dissolved oxygen from a station above the slope off Newport, OR in March–April used in computing offshore initial condition fields for various model simulations. Offshore waters in 2002 had significantly lower DO concentrations at all depths than the LTOP climatology and the 2006 observations. Not shown in this figure is the NCOM-2008 DO profile estimated from the regression analysis against NO_3, which had significantly higher concentrations than all the profiles shown, especially at depth.

9.3.3 Model–Data Comparisons

Detailed comparisons of the physical model simulations with observations are described for 2002 in Koch et al. (2010). There was good model–data agreement on the structure and seasonal development of surface and depth-averaged velocities over the shelf and in the offshore transition zone, the structure and development of the upwelling SST front, the separation and offshore intensification of the upwelling jet, and the 3-dimensional density field.

For the ecosystem components, we compare the modeled vertical profiles of NO_3 and DO to GLOBEC-LTOP July 2002 vertical profiles (e.g., 3.5 months after the start of the simulation). Figure 9.7 shows vertical profiles of NO_3 and DO along

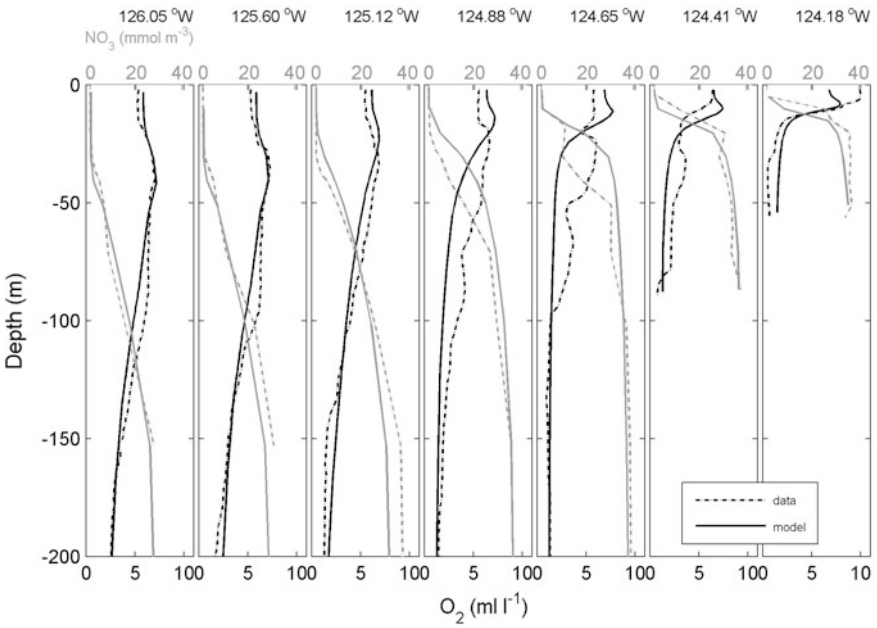

Fig. 9.7 Vertical profiles of NO_3 (mmol N m^{-3}; *gray*) and dissolved oxygen (ml L^{-1}; *black*) from the model (*solid lines*) and observations (*dotted-dashed lines*) along the Newport Hydrographic transect (Fig. 9.1, 44.65° N) during 10–12 July 2002. Leftmost panel is 85 miles offshore; *rightmost two panels* are 15 miles and 5 miles from shore

the NH line for 10–12 July 2002. There is a very good agreement between modeled and observed NO_3 and DO at offshore deep locations and on the shelf. There is a region over the continental slope (NH25, NH35), where the NO_3 and DO profiles from the model underestimate DO and overestimate NO_3 at intermediate depths, although at both shallower and deeper depths the model–data agreement is quite good.

9.4 Description of Oregon Shelf Hypoxia in 2002 and 2006

The patterns of seasonal hypoxia development in summer from the model simulations of 2002 and 2006 are illustrated by showing monthly averaged, cross-shelf vertical sections of dissolved oxygen for the Newport line (Fig. 9.8), monthly maps of the minimum dissolved oxygen concentration (Fig. 9.9), and time–latitude plots

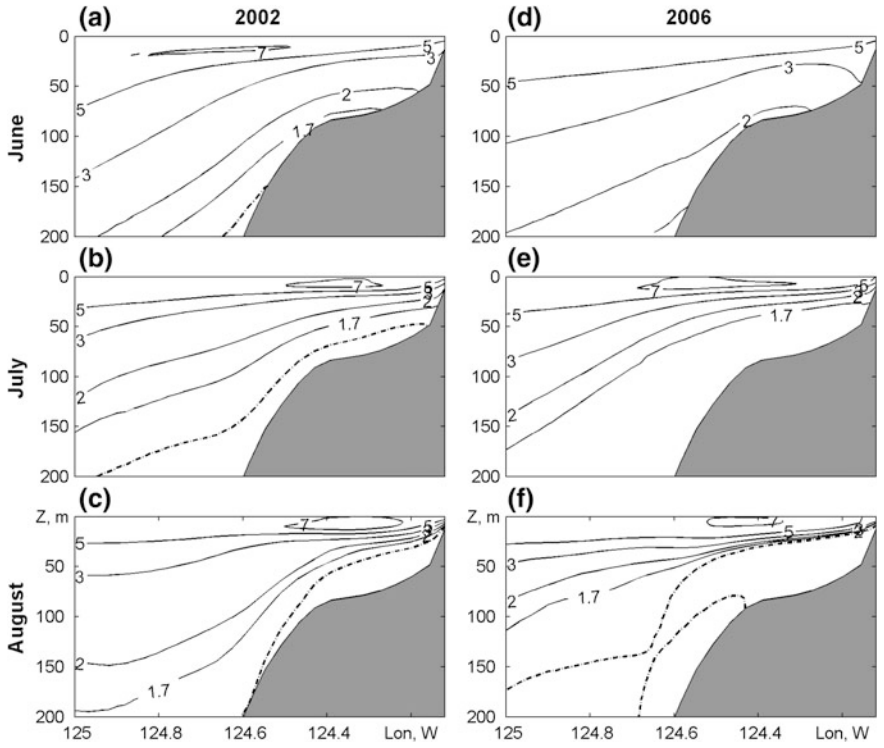

Fig. 9.8 ROMS-CTZ modeled dissolved oxygen concentrations (ml L^{-1}) on a Newport Hydrographic cross-shelf transect averaged from twice-daily values for all days in June (**a**, **d**), July (**b**, **e**) and August (**c**, **f**) of 2002 (**a**–**c**) and 2006 (**d**–**f**). The *dash-dot contour* shows the hypoxic threshold at 1.43 ml L^{-1}

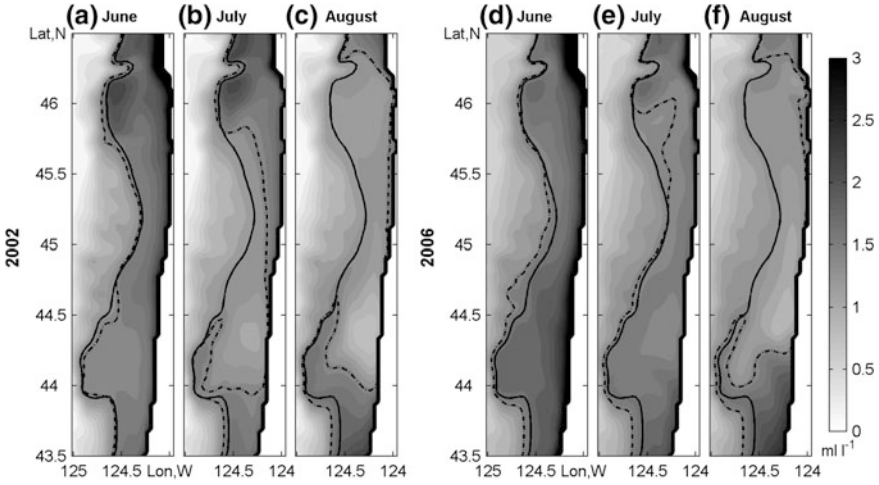

Fig. 9.9 Minimum DO concentration (ml L^{-1}) in the water column over the continental shelf for June (**a**, **d**), July (**b**, **e**), and August (**c**, **f**) of 2002 (**a**–**c**) and 2006 (**d**–**f**). *Heavy solid line* is the 200 m isobath. *Dashed line* is the location of the hypoxia threshold (1.43 ml L^{-1}) near the *bottom*. Minimum DO values were taken over vertical axis for every horizontal grid cell from daily averages of twice-daily outputs. Then, monthly averages for each horizontal grid cell were calculated

that show the seasonal cross-shelf extent of hypoxia (Fig. 9.10). Both monthly averages and minimums were calculated from daily averages of twice-daily outputs. All these results are based on the base case simulations: for 2002 simulation BC2 (Base Case-2002) and for 2006 simulation BC6 (see Table 9.2 for details).

In June 2002, the monthly averaged DO showed bottom hypoxia, but only at bottom depths exceeding 150 m (Fig. 9.8). Modeled hypoxia was severe from offshore to inshore in July and August, but temporally and spatially intermittent (Fig. 9.10), with inner- and mid-shelf bottom regions in both months having <1 ml L^{-1} DO, and the monthly averaged bottom DO being hypoxic across the entire Newport shelf (Fig. 9.8b, c). Grantham et al. (2004) reported that the few observations of inner-shelf bottom DO from mid-July to mid-September of 2002 all indicated severe bottom hypoxia. Newport transects at 44.65° N from the model reveal that inner- and mid-shelf bottom waters became hypoxic in July (Fig. 9.9b), with most of the shelf width experiencing bottom hypoxia. On average, about 20–30% of the shelf off Newport was hypoxic most days in July, gradually increasing from the first shelf hypoxia observed in mid-June (Fig. 9.10a). The model suggests that hypoxia appeared earliest at Newport and further south (near Heceta Bank) and was most severe and extended furthest off the bottom (35–40 m) in August where the bottom depths were 100 m or less (Fig. 9.8). North of 45° N, the model shows that hypoxia was not present on the inner-shelf in July (Fig. 9.9b) and was not widespread across the shelf until August (Figs. 9.9c and 9.10a).

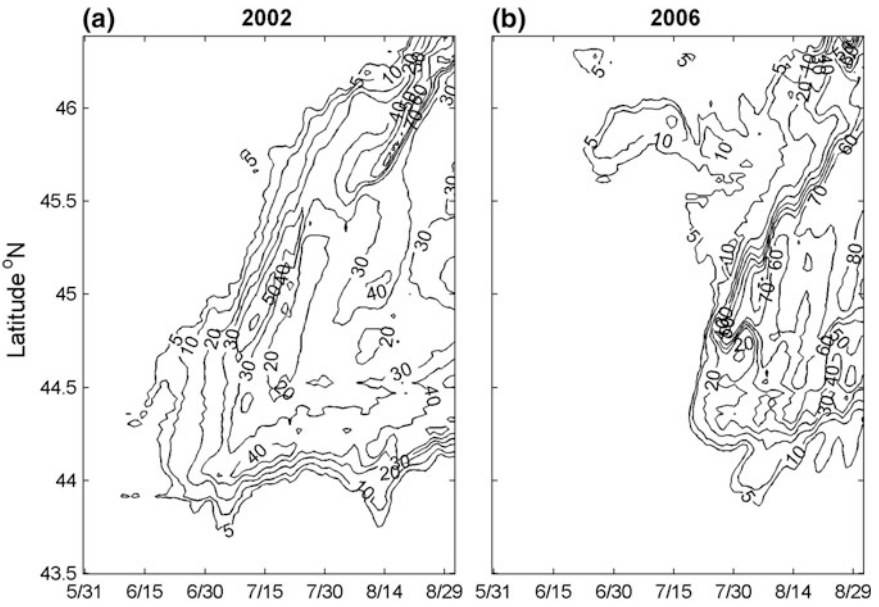

Fig. 9.10 Percentage of the latitudinal cross-shelf area (to 200 m isobath) experiencing hypoxia (DO < 1.43 ml L^{-1}) as a function of time for the base case model simulations in the sensitivity analysis (see Table 9.2): BC2 (**a** 2002) and BC6 (**b** 2006). Daily averages of twice-daily values were used

Table 9.2 Initial and open boundary conditions for dissolved oxygen (DO) and nitrate (NO_3) concentrations for four model simulations in 2002 and one in 2006 that comprised the sensitivity analysis. Two letter case prefixes BC, UI, CI and UB indicate the base case, unmodified initial conditions, climatological initial conditions and unmodified boundary conditions, respectively. One digit Case suffix 2 and 6 indicate the summer 2002 and 2006 simulations, respectively. For all four 2002 simulations, initial and boundary physical conditions are from NCOM-2002; initial and boundary biology conditions are from NCOM-2008, because NCOM-2002 did not include ecosystem variables, and wind forcing in 2008 was most similar to wind forcing in 2002; atmospheric wind forcing is from COAMPS-2002, and heat fluxes are from NCEP-2002. The single 2006 simulation (BC6) used NCOM-2006 for providing both biological and physical initial and boundary conditions, and NAM-2006 provided the wind and heat flux estimates. JP-2006 as the source for DO means in situ DO observations obtained by Jay Peterson (Oregon State University) in early spring in 2006 were used to initialize DO. See text for details on other abbreviations/methods for specifying initial and boundary conditions

Year	Case	Initial conditions		Boundary conditions	
		Dissolved oxygen (DO)	Nitrate (NO_3)	Dissolved oxygen (DO)	Nitrate (NO_3)
2002	BC2	LTOP-2002	LTOP-2002	N:O on mod NCOM-2008	NCOM:LTOP
	UI2	N:O on NCOM-2008	NCOM-2008	N:O on mod NCOM-2008	NCOM:LTOP
	CI2	LTOP-clim	LTOP-clim	N:O on mod NCOM-2008	NCOM:LTOP
	UB2	LTOP-2002	LTOP-2002	N:O on NCOM-2008	NCOM-2008
2006	BC6	JP-2006	LTOP-clim	N:O on mod NCOM-2006	NCOM:LTOP

Modeled hypoxia in 2006 exhibited a different temporal–spatial development from that shown for 2002. Although there was a short period of hypoxia locally near 46° N beginning in June (Fig. 9.10b), widespread along-shelf hypoxia did not occur until late July, and severe and spatially extensive hypoxia occurred only in August (Fig. 9.9f). Model results showed that about 60–80% of the shelf had bottom hypoxia in August, and almost 50% of the shelf volume of water had DO concentrations below the hypoxia threshold in late August, especially between Newport and 46° N.

9.5 Sensitivity Analysis Experiment in 2002

To examine the relative importance of variable NO_3 and DO initial and boundary conditions for summer hypoxia development on the Oregon shelf in 2002, we conducted a set of controlled sensitivity simulations. Table 9.2 provides details of ecosystem and physical initial and open boundary conditions, including atmospheric forcing, used in the numerical experiment. The base case simulation, BC2 (2002; BC for base case), described in the previous section, used the most realistic initial and open boundary conditions available. NO_3 and DO initial conditions for BC2 are from 2002 data collected by the US GLOBEC Northeast Pacific Long-Term Observation Program (LTOP), that sampled off the coast of Oregon from 1997–2004 (Batchelder et al. 2002). Three other model settings, which varied in either their initial conditions or the boundary conditions, were simulated to assess how much the results differ from the BC2 simulation. In simulation UI2 (2002; UI for unmodified initial conditions), the boundary conditions for NO_3 and DO are as in BC2, but initial conditions for NO_3 and DO are estimated from the unmodified NO_3 NCOM fields. For simulation CI2 (2002; CI for climatological initial conditions), a multi-year (1997–2004) climatology of DO and NO_3 derived from GLOBEC-LTOP sampling in April provided the initial conditions for DO and NO_3, and the boundary conditions were identical to those as in BC2. Simulation UB2 (2002; UB for unmodified boundary conditions) uses the same initial conditions as BC2 and boundary DO and NO_3 conditions from unmodified NCOM fields.

9.5.1 Analysis of the Basic Simulation in the Sensitivity Experiment

Summer hypoxia development on the shelf and its characteristics were compared among the simulations in the sensitivity experiment by computing the number of days each month (June, July and August) for each location that the bottom DO concentration was below the hypoxic threshold (Fig. 9.11).

As was noted from the analysis of BC2 in Fig. 9.10a, hypoxic waters in 2002 first appear on Heceta Bank in June. Heceta Bank is a relatively shallow shelf area surrounded by deeper bathymetry; hypoxia also occurs near 44–44.5° N, where the shelf is broad (Fig. 9.9). The along-shore coastal jet, which tends to follow the shelf edge, veers offshore near Heceta Bank (Koch et al. 2010). Circulation on the bank is slow, and recirculation and meanders are common and provide long-residence times for phytoplankton growth. Concentrations of phytoplankton (measured by chlorophyll) were high on the bank in 2002 (Grantham et al. 2004). Some of this phytoplankton is consumed by zooplankton, and some sinks to the bottom as phytodetritus. Near the bottom, DO is reduced by detritus decomposition and ammonium oxidation.

Due to the long-residence time of water on the bank, bottom waters in the BC2 simulation are more likely to become hypoxic. On the bank, bottom DO concentrations are hypoxic for 12–20 days in June (Fig. 9.11a, left panel). In July, hypoxic

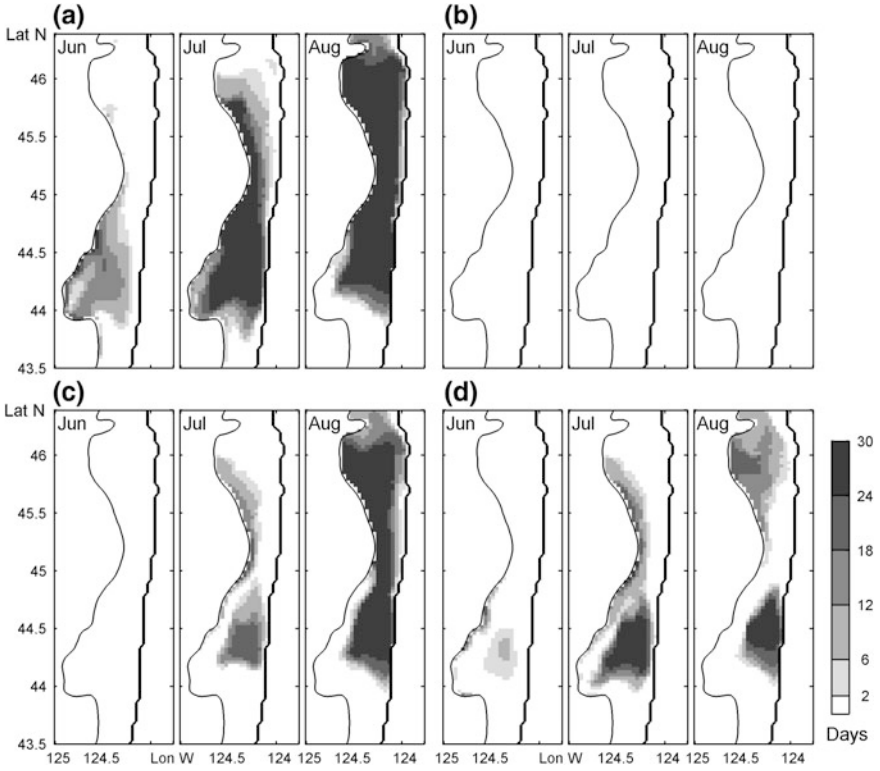

Fig. 9.11 Number of days during the month when bottom DO concentrations were less than the hypoxic threshold (i.e., <1.43 ml L^{-1}) in summer of 2002 for the model simulations **a** BC2, **b** UI2, **c** CI2, **d** UB2 (Table 9.2). The coastline is the *heavy dark line* on the *right side* of *each panel*; the shelf edge (200 m isobath) is the *thin line* on the *left side* of *each panel*. Daily averages of twice-daily values were used in determining whether a given day was hypoxic or not

conditions in the BC2 model simulation expanded northward along the shelf break and hypoxic waters occupied all of Heceta Bank, from the shelf break to the coast, with much of the bank experiencing bottom hypoxia through the entire month (Fig. 9.11a, middle panel). Inner-shelf waters are affected by hypoxia north to almost 45° N. This northward expansion of hypoxia from June to July is not due to advection, which is from north to south, but rather to delayed accumulation of phytodetritus due to weaker bloom and stronger along-shore currents where the shelf is narrower. In August, bottom hypoxia occurs nearly every day along the entire shelf from 44–46.5° N (Fig. 9.11a, right panel). The exception is the offshore and southern parts of Heceta Bank that are no longer hypoxic as a result of northward advection of higher DO concentration waters (analysis not shown).

9.5.2 *Sensitivity Simulations with Modified Initial Conditions*

When initial DO and NO_3 conditions are altered from the most realistic values to conditions derived from unmodified NCOM fields, the results (simulation UI2, Table 9.2) do not show development of hypoxia on the Oregon shelf (Fig. 9.11b). The reasons why hypoxia does not develop in this simulation are basically twofold. First, advection of high (overestimated) DO offshore waters onto the shelf might buffer the decline in DO due to biological processes sufficiently such that the hypoxia threshold is not exceeded. Second, the deeper than normal nitrocline from the NCOM fields may inhibit upwelling of NO_3 onto the shelf, which reduces the total phytoplankton production and the biological oxygen demand when the phytodetritus remineralizes near the bottom.

The CI2 simulation that uses NO_3 and DO from the LTOP multi-year climatology for the initial April conditions (CI2; Table 9.2) produces shelf hypoxia (Fig. 9.11c), though there are substantial spatial and temporal differences from the BC2 simulation (Fig. 9.11a). Bottom hypoxia develops along the shelf break north of 45° N and, again, in the Heceta Head transect (see Fig. 9.4) only in July, thus being delayed about one month (Fig. 9.11c, middle panel). In August, distribution of bottom hypoxic waters over the shelf is similar to BC2, although there are subtle differences in the southward extent of hypoxia along the shelf break (Fig. 9.11c, right panel).

9.5.3 *Sensitivity Simulation with Modified Boundary Conditions*

The UB2 simulation shows that DO and NO_3 conditions at the open boundaries influence summer hypoxia on the shelf. The shelf hypoxia for the simulation using

unmodified NCOM fields at the open boundaries (UB2, Table 9.2) is shown in Fig. 9.11d. Bottom hypoxia appears first along the shelf break and on Heceta Bank in June (Fig. 9.11d, left panel), but later than in simulation BC2. The development and propagation of bottom hypoxia in July and August resemble those of BC2, but the spatial extent and duration of bottom hypoxia are considerably reduced (Fig. 9.11d, middle and right panels). Even with unrealistically high DO and low NO_3 concentrations at the open boundaries, UB2 simulated the beginning of hypoxia better than did CI2 that had more realistic boundary conditions, but used climatological initial conditions. This result suggests that having accurate initial conditions for DO and NO_3 within the model domain in early spring of 2002 was important in replicating the progression of observed summer 2002 hypoxia.

In our model domain, boundary effects might result from conditions on any of the open northern, southern or western boundaries. A simulation (not shown) where DO and NO_3 concentrations at the open western boundary were set to zero showed no difference from simulation BC in the development of bottom hypoxia on the shelf. The western boundary of the model is too distant (400 km from the coast), and the cross-shelf flow velocities are too slow to influence DO and NO_3 concentrations on the shelf within the five month simulation period. Thus, the effects of DO and NO_3 entering the shelf subdomain through the perimeter ultimately came from either the northern or southern open boundaries. This is not surprising given the much greater magnitude of along-shore flows (especially from the north) than cross-shelf flows in the California Current System.

9.6 Role of Physical and Biological Drivers

To determine the relative importance of physical and biological factors to the development of summer hypoxia on the Oregon shelf in 2002 and 2006, we integrate the DO budgets for each model process for the entire water column for the entire simulation (April 1–September 1) and for the summer (June 1–September 1) only over the shelf subdomain (Fig. 9.12). The results of base case simulations BC2 and BC6 are used. The contribution of each process to total oxygen concentration is summarized in Table 9.3. The net change of DO in modeled shelf waters for April–August 2006 is estimated as a loss of $4.7 * 10^{15}$ ml O_2 (hereafter in this paragraph we provide volumes in km^3 ($1\ km^3 = 10^{15}$ ml)), which is equivalent to a decrease of 3.0 ml L^{-1} through the entire shelf. This is 2.5 times higher than the decrease in 2002 (1.8 km^3 O_2; Table 9.3).

Although oxygen reduction due to biological sink terms (organic remineralization) is important in deeper layers in both years, the net biological effect on dissolved oxygen overall, considering the full water column, is positive and large due to the large O_2 production by phytoplankton photosynthesis in the photic zone (ca. 8.7 km^3 O_2 in both 2002 and 2006, Table 9.3). The net effect of horizontal advection is to decrease DO on the shelf through off-shelf advection during upwelling of high DO surface waters (due to photosynthesis; e.g., biological source

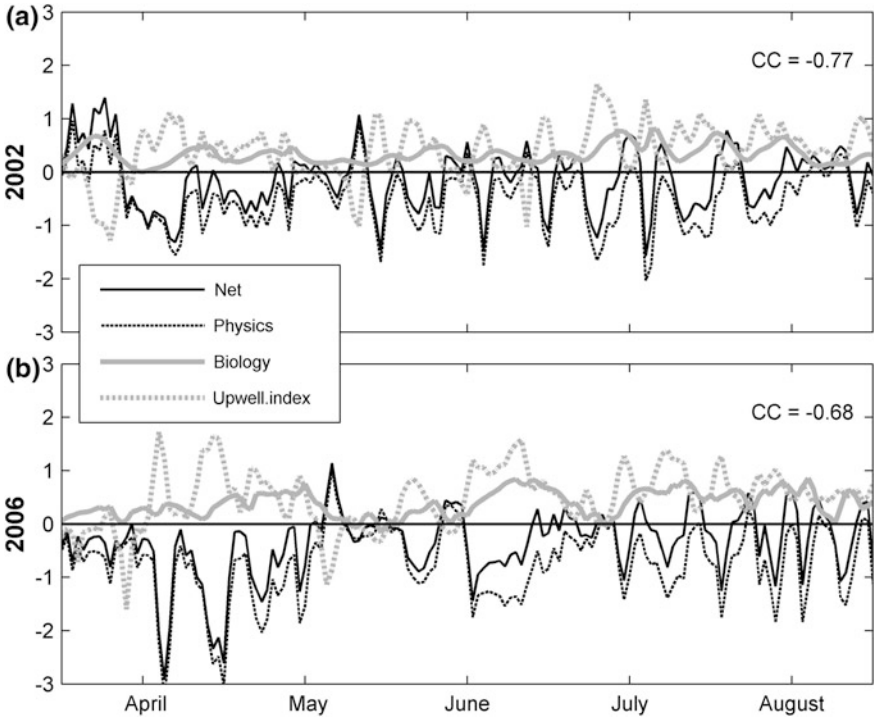

Fig. 9.12 Simulated physical (*dash black*), biological (*solid gray*) and net (*solid black*) fluxes of dissolved oxygen integrated over the shelf ($\times 10^9$ ml s^{-1}) along with the zonal integrated upwelling index (NOAA, S. Pierce; $\times 3000$ m^3 s^{-1}) for **a** 2002 and **b** 2006. Upwelling index/physical flux correlations (CC) are shown

Table 9.3 Dissolved oxygen (DO) shelf budgets (ml $O_2 \cdot 10^{15}$ (=1 km^3)) in 2002 and 2006 due to different processes: advection, diffusion, air-sea flux, biological production and loss, net physical, net biological and total net change during the entire integration period April–August and during the summer (June–August) only. Net terms are highlighted in bold

Factor/Time interval	April–August 2002	April–August 2006
Advection	−3.1	−5.7
Diffusion	−2.0	−2.9
Air-sea flux	−1.1	−1.1
Physical net	**−6.2**	**−9.7**
Biological source	8.7	8.7
Biological sink	−4.3	−3.7
Biological net	**4.4**	**5.0**
Total net	**−1.8**	**−4.7**
Factor/time interval	June–August 2002	June–August 2006
Physical net	**−4.2**	**−5.2**
Biological net	**3.0**	**3.5**
Total net	**−1.2**	**−1.7**

in Table 9.3) and deep intrusions of low DO waters onto the shelf from offshore. About 12% of the biologically produced oxygen near the surface is lost by outgassing of oxygen from supersaturated surface waters to the atmosphere. The physical mechanisms of DO reduction, especially through horizontal advection and diffusion, are responsible for losses of 6.2 km^3 O_2 in 2002 and 9.7 in 2006 (Table 9.3) and are the critical factors for the overall decline of DO on the shelf.

Since the DO change due to biological processes was similar in 2002 and 2006, the large difference between years in net DO change is ultimately due to the difference in physical forcing. In 2002, the loss of DO occurred predominantly in June–August, whereas in 2006 two-thirds of the net DO loss occurred during very strong upwelling events in April and May (Fig. 9.1). Time series of the DO fluxes (physical, biological and net) integrated over the entire shelf volume clearly show greater net biological production of DO in June–August (67–70% of total) than earlier, and the close matching of physical and net DO fluxes in both years (Fig. 9.12). There is a strong negative correlation between DO physical flux and upwelling index in both years: −0.77 in 2002 and −0.68 in 2006 (Fig. 9.12). This relationship is explained by a simple conceptual model of upwelling, wherein relatively high DO surface waters are advected offshore past the shelfbreak, while deeper waters having low dissolved oxygen are advected onshore from beyond the shelf. This circulation pattern would decrease DO concentration in shelf waters. In contrast, deeper waters advected onto the shelf would have high nutrient concentrations and with injection into the inner-shelf euphotic zone would facilitate enhanced phytoplankton growth and DO production. Considering the full depth-integrated water column on the shelf, the physical processes dominate over the biological processes in controlling the total oxygen content. These budget results are consistent with model results of Siedlecki et al. (2015) for whole water column integrations of the Oregon and Washington shelves.

Whole water integrations, as done by us and Siedlecki et al. (2015), could be supplemented by examining the water column partitioned into the euphotic DO production zone and a deeper zone dominated by remineralization processes, where each has biological and physical sources and sinks of dissolved oxygen. We did not do vertically partitioned DO budgets for this analysis.

The documented differences in hypoxia timing, spatial distribution and severity in 2002 and 2006 could be explained as follows. On the one hand, with the comparable rates of biological net oxygen production in both years, physical oxygen removal (mainly due to upwelling) rate in 2006 is about 1.5 higher resulting in net oxygen loss rate being 2.5 higher than in 2002 (Table 9.3 and Fig. 9.12). On the other hand, initial oxygen concentrations in early April of 2002 are essentially lower than in 2006 (Fig. 9.6), which provides a head start for shelf waters DO concentration to drop below hypoxic level as early as in mid-June. In 2006, despite strong (especially in April–May) upwelling, the initial DO concentration in shelf waters is relatively high, and it takes as much as 3.5–4 months to develop strong shelf hypoxia. From that point on (2nd half of July–August), hypoxia development

in 2006 seems to be more rapid and ubiquitous than in 2002, which is well documented in Fig. 9.10, and is also supported by observations in September (outside of our model integration interval) on Fig. 9.2.

9.7 Discussion and Conclusions

Our results that indicate the Heceta Bank region of the Oregon shelf is a hotspot for hypoxia are consistent with the analysis of observations reported by Connolly et al. (2010) and with model simulations conducted by Siedlecki et al. (2015). There is substantial year-to-year variability in the spatial and temporal extent and intensity of hypoxia (Siedlecki et al. 2015) in the Pacific Northwest. Their model showed three regions of the Oregon–Washington coast that had persistent hypoxia in late-summer simulations of three years, which included Heceta Bank as well as two regions in Washington, one of which was the Juan de Fuca Eddy (JdFe) region offshore of the Strait of Juan de Fuca. Both Heceta Bank and JdFe are known to be regions where water residence times are relatively long because of local recirculation flows (Barth et al. 2005; Hickey and Banas 2003). Both regions had high vertically integrated water column organic matter respiration (Seidlecki et al. 2015).

The coupled biophysical model used in this study demonstrated skill in reproducing the physical and biological processes that govern Oregon shelf summer hypoxia. With realistic and controlled sensitivity simulations we were able to understand the relative contributions of ocean physics and ecological processes in creating regional hypoxia on the Oregon shelf. The sensitivity analysis demonstrated the importance of having accurate ecosystem boundary and early spring initial conditions, especially the latter, for accurate hindcasting of summer–autumn oxygen on the Oregon shelf. Unrealistically high initial DO and low NO_3 conditions in spring 2002 (from NCOM derived fields) prevented or significantly delayed bottom hypoxia development. We also showed that when lacking year-specific data for specifying the initial conditions of NO_3 and DO, a simulation initialized with a 7-year climatological average conditions was able to reveal the spatial pattern of hypoxia, although not the full temporal development (the climate scenario had weaker and delayed hypoxia). DO changes due to biological processes (photosynthesis, respiration, remineralization) are large, although physical processes, mostly horizontal advection of low DO in the bottom boundary layer associated with upwelling, are most responsible for the net reduction in DO in spring–summer and the onset of bottom hypoxia in summer on the Oregon shelf.

For realistic modeling of shelf hypoxia, it is critical to have accurate estimates of the initial and boundary conditions. These are often provided by larger-scale numerical models or, in cases where they are available, by recent ocean observations of the relevant parameters. In our modeling, initial and boundary values of NO_3 and DO concentrations are critical for evaluating hypoxia development. Many large-scale coupled physical–biological models do not provide sufficiently realistic DO and NO_3 information essential to force higher spatial resolution (local-regional)

models for hindcasting (or forecasting) the intensity, duration and spatial patterns of hypoxia on the Oregon shelf. No available regional model simulations in hindcast, nowcast or forecast mode are presently able to provide the external boundary conditions and forcing required for higher resolution coastal models, like the model described here, that focus on dissolved oxygen dynamics. An alternative to downscaling from larger-scale models might be more intensive in situ sampling, which provides directly measured DO and NO_3. Often, the limited vertical resolution of the coarser resolution larger-domain models is insufficient to provide fine enough vertical information to the local model to resolve the depth of the oxygen minimum zone (OMZ) offshore, or the potential shallowing of it through recent decades. In regions where OMZ offshore has shown to be shallowing, it is important to include these changes by prescription or by modeling to enable realistic hindcasting and forecasting of hypoxia on continental shelves, which has direct effects on marine biota and livelihoods.

Appendix A. Oxygen Formulation

The dissolved oxygen dynamics in our ecosystem model is governed by the following equation:

$$\frac{\partial O_2}{\partial t} = V_m f(I)\left\{\frac{NO_3}{K_u + NO_3} e^{-\psi NH_4} r_{O_2:NO_3} + \frac{NH_4}{K_u + NH_4} r_{O_2:NH_4}\right\} P$$

$$- 2\Omega NH_4 - \Gamma r_{O_2:NH_4} Z - \varphi r_{O_2:NH_4} D + Q_{ge}(O_{2sat} - O_2)$$

where P is phytoplankton, Z is zooplankton, D is detritus, $V_m = 1.5\ \mathrm{d}^{-1}$ is phytoplankton maximum uptake rate, *f(I)* is light limitation (see Spitz et al. 2005 for details), $\psi = 1.46\ (\mathrm{mmol\ N\ m}^{-3})^{-1}$ is NH_4 inhibition parameter, $\Omega = 0.25\ \mathrm{d}^{-1}$ is NH_4 oxidation coefficient, $\Gamma = 0.1\ \mathrm{d}^{-1}$ is zooplankton specific excretion and mortality rate, $\varphi = 0.1\ \mathrm{d}^{-1}$ is detritus decomposition rate, $r_{O_2:NO_3}$ and $r_{O_2:NH_4}$ are oxygen-nitrate and oxygen-ammonium conversion parameters, respectively; $Q_{ge} = \frac{K\nu_{O_2}}{\Delta zn}$, where Δzn is the height of the top cell and $K\nu_{O_2} = 0.31u^2\sqrt{660/S_c}$ is the gas transfer coefficient with u being the average wind speed and S_c being Schmidt number calculated after Keeling et al. (1998): $S_c = 1638.0 - 81.83T + 1.483T^2 - 0.008004T^3$; $O_{2sat} = e^A 1000/22.9316$ is the saturation concentration of oxygen with $A = 2.00907 + 3.22014TS + 4.05010TS^2 + 4.94457TS^3 - 0.256847TS^4 + 3.88767TS^5 + S(-0.00624523 - 0.00737614TS - 0.0103410TS^2 - 0.00817083TS^3) - 4.88682 \cdot 10^{-7}S^2$, where $TS = \ln((298.15 - T)/T_k)$, T is in Celsius, T_k in Kelvin (after Garcia and Gordon 1992).

References

Bakun A (1990) Global climate change and intensification of coastal ocean upwelling. Science 247:198–201

Barth JA, Pierce SD, Castelao RM (2005) Time-dependent, wind-driven flow over a shallow midshelf submarine bank. J Geophys Res 110:C10S05. doi:10.1029/2004JC002761

Batchelder HP, Barth JA, Kosro PM, Strub PT, Brodeur RD, Peterson WT, Tynan CT, Ohman MD, Botsford LW, Powell TM, Schwing FB, Ainley DG, Mackas DL, Hickey BM, Ramp SR (2002) The GLOBEC Northeast Pacific California Current system program. Oceanography 15(2):36–47

Castelao RM, Barth JA (2005) Coastal ocean response to summer upwelling favorable winds in a region of alongshore bottom topography variations off Oregon. J Geophys Res 110:C10S04. doi:10.1029/2004JC002409

Chan R, Barth JA, Lubchenco J, Kirincich A, Weeks H, Peterson WT, Menge. BA (2008) Emergence of anoxia in the California Current large marine ecosystem. Science 319:920. doi:10.1126/science.1149016

Connolly TP, Hickey BM, Geier SL, Cochlan WP (2010) Processes influencing seasonal hypoxia in the northern California Current system. J Geophys Res 115:C03021. doi:10.1029/2009JC005283

Crawford WR, Pena MA (2013) Declining oxygen on the British Columbia continental shelf. Atmos Ocean 51:88–103

Diaz RJ, Rosenberg R (2008) Spreading dead zones and consequences for marine ecosystems. Science 321:926. doi:10.1126/science.1156401

Escribano R, Schneider W (2007) The structure and functioning of the coastal upwelling system off south/central Chile. Prog Oceanogr 75:343–346

Garcia HE, Gordon LI (1992) Oxygen solubility in seawater: better fitting equations. Limnol Oceanogr 37(6):1307–1312

Grantham BA, Chan F, Nielsen KJ, Fox DS, Barth JA, Huyer A, Lubchenco J, Menge BA (2004) Upwelling-driven nearshore hypoxia signals ecosystem and oceanographic changes in the Northeast Pacific. Nature 429:749–754

Hickey BM, Banas NS (2003) Oceanography of the US Pacific Northwest coastal ocean and estuaries with application to coastal ecology. Estuaries 26:1010–1031. doi:10.1007/BF02803360

Hodur RM (1997) The naval research laboratory's coupled ocean/atmosphere mesoscale prediction system (COAMPS). Mon Weather Rev 125:1414–1430

Huyer A, Sobey EJC, Smith RL (1979) The spring transition in currents over the Oregon continental shelf. J Geophys Res 84:6995–7011

Kalnay E et al (1996) The NCEP/NCAR 40-year reanalysis project. Bull Am Meteorol Soc 77:437–471

Keeling RF, Manning AC, McEvoy EM, Shertz SR (1998) Methods for measuring changes in atmospheric O_2 concentration and their application in Southern Hemisphere air. J Geophys Res 103:3381–3397

Koch AO, Kurapov AL, Allen JS (2010) Near-surface dynamics of a separated jet in the coastal transition zone off Oregon. J Geophys Res 115:C08020. doi:10.1029/2009JC005704

Levitus S (1982) Climatological atlas of the world ocean. NOAA Professional Paper 13, US Government printing office, Washington DC, 173 pp

Peterson JO, Morgan CA, Peterson WT, Di Lorenzo E (2013) Seasonal and interannual variation in the extent of hypoxia in the northern California Current from 1998-2012. Limnol Oceanogr 58:2279–2292

Shchepetkin AF, McWilliams JC (2003) A method for computing horizontal pressure-gradient force in an oceanic model with a nonaligned vertical coordinate. J Geophys Res 108(C3):3090. doi:10.1029/2001JC001047

Shchepetkin AF, McWilliams JC (2005) The regional ocean modeling system: a split–explicit, free–surface, topography–following coordinate oceanic model. Ocean Model 9:347–404. doi:10.1016/j.ocemod.2004.08.002

Shulman I, Kindle JC, deRada S, Anderson SC, Penta B, Martin PJ (2004) Development of a hierarchy of nested models to study the California Current system. Estuarine and coastal modeling. In: Malcolm L, Spaulding PE (eds) Proceedings of the 8th international conference on estuarine and coastal modeling. American Society of Civil Engineers, Reston, Va, pp 74–88

Siedlecki SA, Banas NS, Davis KA, Giddings S, Hickey BM, MacCready P, Connolly T, Geier S (2015) Seasonal and interannual oxygen variability on the Washington and Oregon continental shelves. J Geophys Res Oceans 120. doi:10.1002/2014JC010254

Spitz YH, Allen JS, Gan J (2005) Modeling of ecosystem processes on the Oregon shelf during the 2001 summer upwelling. J Geophys Res 110:C10S17. doi:10.1029/2005JC002870

Strub PT, Batchelder HP, Weingartner TJ (2002) U.S. GLOBEC Northeast Pacific program: overview. Oceanography 15:30–35

Ueno H, Yasuda O (2003) Intermediate water circulation in the North Pacific subarctic and northern subtropical regions. J Geophys Res 108(C11):3348. doi:10.1029/2002JC001372

Wetz JJ, Hill J, Corwith H, Wheeler PA (2004) Nutrient and extracted chlorophyll data from the GLOBEC long-term observation program, 1997–2004. Data report 193, COAS reference 2004-1 (Revised June 2005 [to include improved 2003 and 2004 data]). http://nepglobec.bco-dmo.org/reports/ccs_cruises/GLOBEC_nutchl_datareport_7_06_hpb.pdf

Wheeler PA, Huyer A, Fleischbein J (2003) Cold halocline, increased nutrients and higher chlorophyll off Oregon in 2002. Geophys Res Lett 30. ISSN: 0094-8276. doi:10.1029/2003GL017395